J. Fluid Mech. (1973), *vol.* 60, *part* 1, *pp.* 1–17
Printed in Great Britain

On the Weis-Fogh mechanism of lift generation

By M. J. LIGHTHILL

Department of Applied Mathematics and Theoretical Physics,
University of Cambridge

(Received 27 March 1973)

Weis-Fogh (1973) proposed a new mechanism of lift generation of fundamental interest. Surprisingly, it could work even in inviscid two-dimensional motions starting from rest, when Kelvin's theorem states that the total circulation round a body must vanish, but does *not* exclude the possibility that if the body breaks into two pieces then there may be equal and opposite circulations round them, each suitable for generating the lift required in the pieces' subsequent motions! The 'fling' of two insect wings of chord c (figure 1) turning with angular velocity Ω generates irrotational motions associated with the sucking of air into the opening gap which are calculated in § 2 as involving circulations $-0{\cdot}69\Omega c^2$ and $+0{\cdot}69\Omega c^2$ around the wings when their trailing edges, which are stagnation points of those irrotational motions, break apart (position (f)). Viscous modifications to this irrotational flow pattern by shedding of vorticity at the boundary generate (§ 3) a leading-edge separation bubble, and tend to increase slightly the total bound vorticity. Its role in a three-dimensional picture of the Weis-Fogh mechanism of lift generation, involving formation of trailing vortices at the wing tips, and including the case of a hovering insect like *Encarsia formosa* moving those tips in circular paths, is investigated in § 4. The paper ends with the comment that the far flow field of such very small hovering insects should take the form of the exact solution (Landau 1944; Squire 1951) of the Navier–Stokes equations for the effect of a concentrated force (the weight mg of the animal) acting on a fluid of kinematic viscosity ν and density ρ, whenever the ratio $mg/\rho\nu^2$ is small enough for that jet-type induced motion to be stable.

1. Introduction

Weis-Fogh (1973), in his analysis of the hovering motions of the chalcid wasp *Encarsia formosa* (an economically important parasite used in the biological control of greenhouse aphids), concluded that its performance is markedly superior to that of most hovering animals as a result of lift generation by a mechanism of considerable fundamental interest not previously studied by aerodynamicists. Normal hovering animals beat their wings back and forth in a horizontal plane, preceding each lift-beat with a wing rotation that allows always the same leading edge to move forwards at an angle of incidence appropriate to a relatively high lift coefficient. Building up that lift coefficient is, however, delayed by the Wagner effect: that is, the time required for vorticity shedding from the trailing edge to generate the necessary circulation around the wing

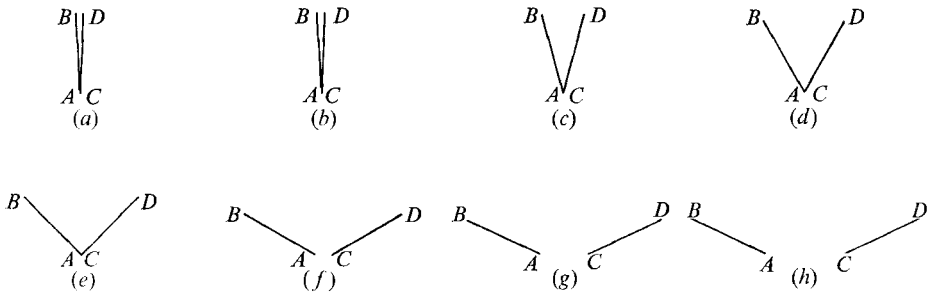

FIGURE 1. Sequence of motions of the wings of *Encarsia formosa*, shown in section by a mid-span vertical plane on the dorsal side of the insect's erect body. In positions (*a*) and (*b*) the wings are momentarily at rest after the 'clap'; positions (*b*)–(*f*) exhibit the 'fling' motion; the wings break apart at (*f*) and in (*f*), (*g*) and (*h*) exhibit normal flight movement.

(Wagner 1925). *E. formosa* precedes each beat with a special movement (the 'clap and fling') which, as Weis-Fogh argues, may cause the necessary circulation to be generated immediately and avoid any delay in the build-up of maximum lift. High-speed photography was needed to observe the details of these movements, at a wing-beat frequency around 400 Hz.

The Weis-Fogh mechanism, like the Wagner effect, can be described in terms of a purely two-dimensional flow: a description reasonably appropriate as each of the animal's wings has an aspect ratio around 5. This paper gives a quantitative analysis of the Weis-Fogh mechanism in terms of two-dimensional flow theory, but also offers qualitative comments on three-dimensional aspects of the flow patterns in the concluding section, § 4.

A particularly remarkable feature of the mechanism is that Weis-Fogh (1973) was able to describe it approximately in terms of a purely *inviscid* two-dimensional flow. This flow is calculated in § 2 below prior to the investigation of viscous-flow corrections in § 3. It is surprising that a fundamentally new mechanism of lift generation in inviscid two-dimensional flow should be discovered six decades after the work of Prandtl, Zhukovski, Kutta and Lanchester.

The Weis-Fogh mechanism works, furthermore, for a fluid of zero viscosity: not simply in the limit of vanishing viscosity when thin Prandtl boundary layers shed Lanchester vortices at sharp trailing edges where the Kutta–Zhukovski condition is satisfied. To be sure, for inviscid two-dimensional flow the doctrines of Helmholtz, Stokes and Kelvin tell us that a body starting to move in fluid at rest retains always the same zero circulation of fluid around it, preventing the generation of lift on the body (or of any forces except those associated with virtual-mass effects). Those doctrines do not, however, rule out the possibility that when the body *breaks into two pieces* there may be equal and opposite circulations round them, each suitable for generating the lift required in the pieces' subsequent motions!

Figure 1 illustrates in terms of two-dimensional flow the sequence of wing movements comprising the Weis-Fogh mechanism of lift generation. We view 'in elevation' successive positions taken up by sections AB and CD of the two wings in a mid-span vertical plane. The body of the hovering insect is erect with

the head uppermost, and the vertical plane of figure 1 is to the dorsal (back) side of it, halfway between the body itself and the wing tips.

The last three positions (*f*), (*g*) and (*h*) in figure 1 show a motion characteristic of normal hovering flight with both wings moving horizontally at a positive angle of incidence. It will be explained why this motion is enabled by the preceding 'clap and fling' movements to generate maximum lift from the outset; before describing that, however, we note that the normal horizontal motion of the wings is shown as a rectilinear motion in figures 1 (*f*), (*g*) and (*h*), although the wings really move in a horizontal circle around the erect body. Positions showing the horizontal motion at the end of figure 1 proceeding considerably further could properly be depicted only if figure 1 were regarded as a section not by a vertical plane but by a cylindrical surface with the insect's vertical body as axis.

At a certain phase in each wing-beat cycle the insect performs the 'clap': its wings are 'clapped together behind its back' into the contiguous situation shown in the first two positions of figure 1, with leading edges vertically above the trailing edges. We may regard position (*b*) with the surrounding fluid undisturbed as the initial condition for the operation of the Weis-Fogh mechanism, on the grounds that residual eddy motions generated in the clapping process should have been blown far enough away from the wings by then to be uninfluential.

The sequence from figure 1 (*b*)–(*g*), then, shows two wings AB and CD which in the first four positions are touching (with the points A and C coinciding) to form effectively a *single body*. Figure 1 (*f*) shows them breaking apart, while they are fully separate in figure 1 (*g*). The Weis-Fogh mechanism depends on the idea that the rotary movements of AB about A and of CD about C (that is, the 'fling') depicted in positions (*b*)–(*f*) generate a fluid motion which at the moment of figure 1 (*f*) when the wings break apart involves substantial equal and opposite circulations, in the negative sense around AB and in the positive sense around CD, of magnitudes close to those required for generating maximum lift at once in the subsequent horizontal motions. This is the idea that is quantitatively evaluated on inviscid theory in § 2, while modifications due to viscous effects are estimated in § 3. The necessity of such viscous considerations is particularly evident from the low Reynolds numbers involved: around 30 based on a wing chord of 0·22 mm and a leading-edge velocity of 2·2 ms^{-1}. Finally some considerations regarding the idea's application to the fully three-dimensional motions of the insect's wings are sketched in § 4.

2. Two-dimensional inviscid-flow theory

In the two-dimensional model of the 'fling' process depicted in figure 2, the broken line EF represents a plane of symmetry while the lines AB and CD each have length c, the 'chord' of the wings which they represent. They each make an angle α with EF and the 'fling' process is one in which α increases from zero, with the points A and C stationary and coincident, until when α takes a value α_0 (around $\frac{1}{3}\pi$) the wings break apart.

The flow field at each instant of the fling process is, according to inviscid-flow theory, simply the irrotational flow associated with the instantaneous angular

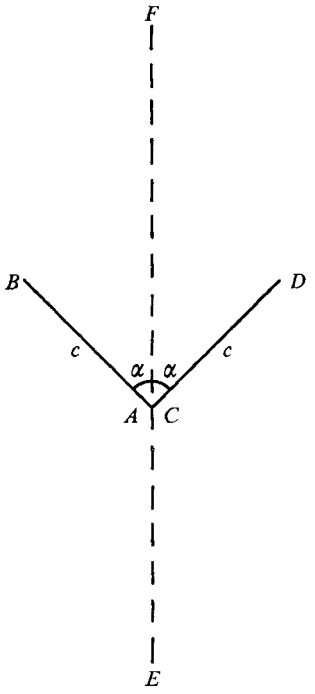

FIGURE 2. Two-dimensional model of the 'fling' process. The points A and C are stationary and coincident and the wings AB and CD rotate about them with angular velocity $\Omega = d\alpha/dt$. The whole motion is symmetrical about the line EF.

velocity $\Omega = d\alpha/dt$ of rotation of the wings. In the present section we calculate this flow, but may note in advance two features of it: there is a stagnation point (zero fluid velocity) on both sides of the corner, and there is a circulation

$$\Gamma = \Omega c^2 g(\alpha) \tag{1}$$

around each wing (in the negative sense around AB and in the positive sense around CD), where $g(\alpha)$ is a computed function of α.

It follows that if the wings break apart when $\alpha = \alpha_0$ and $\Omega = \Omega_0$ the flow field, not involving any motion at the corner where the break occurs, remains unchanged to a close approximation. The circulation around each wing is then $\Omega_0 c^2 g(\alpha_0)$ and on two-dimensional inviscid-flow theory must continue to take that value in the subsequent motion. According to unsteady aerofoil theory this permits substantial lifts on both wings without the need for any vortex shedding. We postpone till § 3 considerations of possible effects modifying this irrotational-flow description, resulting from vortex shedding whether from the leading edges during the fling or from the trailing edges after they break apart, and concentrate here on determining $g(\alpha)$.

In the irrotational flow associated with the motion of figure 2, the line of symmetry EF is a streamline and we investigate the flow to the left of it due to the motion of AB and calculate the resulting circulation Γ. The investigation is carried out (figure 3) in the upper half complex z plane cut from the origin A to

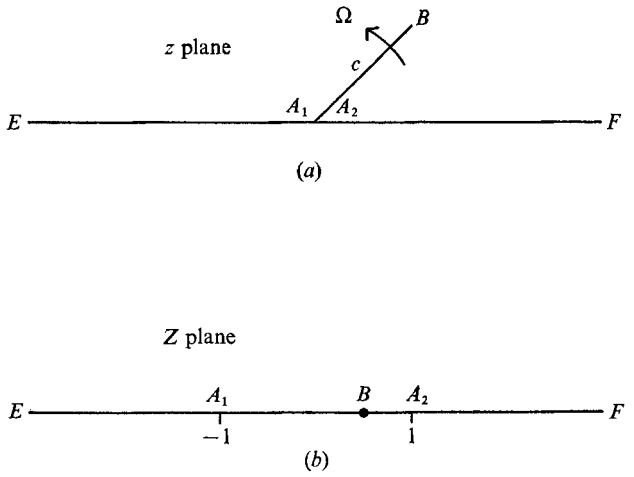

FIGURE 3. Illustrating the complex planes used: the z plane (a), representing the left-hand half of the flow field of figure 2 turned through 90°, is mapped conformally into the upper half Z plane (b).

the point B, where $z = c\,e^{i\alpha}$, with EF the real axis. We distinguish the two corners at A between the wing and the line of symmetry with the designations A_1 and A_2.

A Schwarz–Christoffel conformal mapping from the *cut* upper half z plane to the *uncut* upper half Z plane (figure 3) is defined by

$$\frac{dz}{dZ} = K\left(\frac{Z-1}{Z+1}\right)^{\alpha/\pi}\frac{Z-a}{Z+1} \tag{2}$$

with the term in brackets given argument zero at $Z = \infty$. The points at infinity correspond; the points A_1 and A_2 are mapped into $Z = -1$ and $+1$ respectively, while the need for their positions in the z plane to coincide requires that the integral of (2) from $Z = -1$ to $Z = +1$ vanishes, giving

$$a = 1 - (2\alpha/\pi) \tag{3}$$

as the value of Z at the point B. The quantity $z\,e^{-i\alpha}$ on the wing AB, which represents distance from the origin A, may be written as

$$z\,e^{-i\alpha} = Kf(Z), \quad \text{where} \quad f(Z) = \int_{-1}^{Z}\left(\frac{1-Z}{1+Z}\right)^{\alpha/\pi}\frac{a-Z}{1-Z}dZ, \tag{4}$$

and the condition that it takes the value c at B (where $Z = a$) determines K as

$$K = cf_{\max}^{-1}, \quad \text{where} \quad f_{\max} = f(a) \tag{5}$$

is the maximum of $f(Z)$ for $-1 < Z < 1$.

The stream function ψ, which is the imaginary part of the complex potential w, can be taken as zero on the streamlines EA_1 and A_2F. It is non-zero, however, on the wing AB, along which the normal velocity is Ω times the distance $z\,e^{-i\alpha}$ from A. The rate of change of ψ with this distance is minus this normal velocity, giving

$$\mathrm{Im}\,(w) = \psi = -\tfrac{1}{2}\Omega(z\,e^{-i\alpha})^2 \tag{6}$$

as the boundary condition on both A_1B and A_2B.

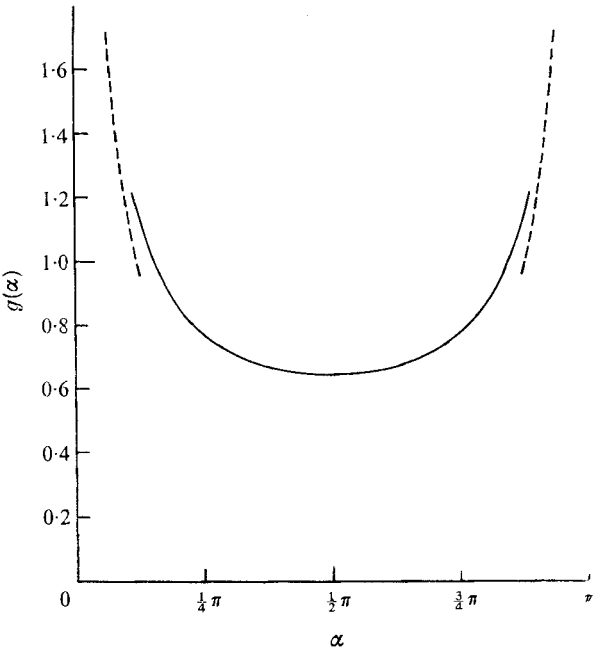

FIGURE 4. The coefficient $g(\alpha)$ in equation (1) for the circulation Γ around AB, as a function of the semi-angle α between the wings given by equation (10), with f and $f_{\max}$ defined in (4) and (5). The broken line represents the approximate formula (12) for small α; a similar approximate form for small $\pi-\alpha$ has been plotted, although it is probably of no practical interest.

The corresponding boundary conditions in the Z plane state that for real Z

$$\mathrm{Im}\,(w) = \begin{cases} -\frac{1}{2}\Omega K^2 f^2(Z) & (-1 < Z < 1), \\ 0 & \text{(otherwise)}. \end{cases} \tag{7}$$

The complex potential $w(Z)$ satisfying these boundary conditions is

$$w = \frac{\Omega K^2}{2\pi}\int_{-1}^{1}\frac{f^2(t)\,dt}{Z-t}. \tag{8}$$

Now the circulation Γ round the wing AB in the negative sense is the change in velocity potential ϕ (the real part of the complex potential w) as we move once round AB from A_1 to A_2, which in the Z plane is from -1 to $+1$. Hence

$$\Gamma = (\Omega K^2/\pi)\int_{-1}^{1}(1-t^2)^{-1}f^2(t)\,dt, \tag{9}$$

which with (5) specifies the coefficient $g(\alpha)$ in (1) as

$$g(\alpha) = \left[\int_{-1}^{1}(1-t^2)^{-1}f^2(t)\,dt\right](\pi f_{\max}^2). \tag{10}$$

This function is easily computed, with results shown in figure 4.

An interesting feature of $g(\alpha)$, not unexpected from its expression (10) as a sort of 'weighted mean', is the flat nature of its graph in the central half of the interval

of possible values of α: thus, $g(\alpha)$ lies between 0·64 and 0·77 when $\frac{1}{4}\pi < \alpha < \frac{3}{4}\pi$ (so that $f(t)$ attains its maximum between $-\frac{1}{2}$ and $\frac{1}{2}$). In fact $0{\cdot}64 < g(\alpha) < 0{\cdot}77$ whenever the angle 2α between the wings is obtuse, and $g(\alpha)$ is varying particularly slowly once that angle has risen to the value 120° ($\alpha = \frac{1}{3}\pi$ with $g(\alpha) = 0{\cdot}69$) at which the separation of the wings is observed.

This is significant not only because it indicates that the circulation $g(\alpha_0)\,\Omega_0 c^2$ is insensitive to the exact value α_0 of α when the wings break apart, but also because it suggests that the pressure difference across the gap is negligible. This difference in pressure between the stagnation points A_1 and A_2 is the difference in values of $-\rho\partial\phi/\partial t$, which is

$$-\rho\, d\Gamma/dt \tag{11}$$

since Γ is the difference in the values of ϕ at A_1 and A_2. On the flat part of figure 4 this quantity should be small.

It may be of interest to note that for very small values of α the quantity $g(\alpha)$ becomes large, approximately like

$$g(\alpha) \sim \frac{1}{4\alpha} + \frac{1}{2\pi}\log\frac{\pi}{\alpha}, \tag{12}$$

of which the graph is shown as a broken line in figure 4. This behaviour can be deduced analytically from (10); alternatively, its physical significance can be seen as follows.

At the start of the 'fling' process, the flow field is dominated by the inrush of air to fill the opening gap between the wings. The volume of air per unit span at a distance less than r from A is αr^2 and the rate of increase of this, namely

$$\Omega r^2, \tag{13}$$

must be achieved (figure 5) by inflow across an arc of small length $2\alpha r$ at a mean speed $\Omega r/2\alpha$. The integral of this from 0 to c is $\Omega c^2/4\alpha$, which explains the leading term in (12) as the large contribution to circulation made by the integral of velocity over the region between the wings where the inflow (13) is spread over a narrow arc.† Outside the region the 'sink' flow into the opening predominates, with an inflow per unit span Ωc^2 coming equally into BD from all directions. In a distance c from A to B the area per unit span over which this inflow is spread drops from $2\pi c$ to $2\alpha c$ (figure 5), and the corresponding change

$$(\Omega c^2/2\pi)\log(\pi/\alpha)$$

in velocity potential accounts for the second term in (12).

Strictly speaking, these questions of what is the flow and the consequent circulation for α small are not important for an inviscid-flow model, on which the circulation at a later instant when $\alpha = \alpha_0$ is determined only by the motion of the boundary and resulting flow at that instant. They have been mentioned here, however, because the modifications by viscous effects studied in § 3 give the

† For the energetics of the 'fling' process, see Weis-Fogh (1973): the essential point is that the combination of elastic system and musculature involved is adapted to operations in which most of the energy expenditure precedes most of the displacement, as is required for small α (though hairs on the wings prevent α from becoming exactly zero) to generate the velocity distribution $\Omega r/2\alpha$.

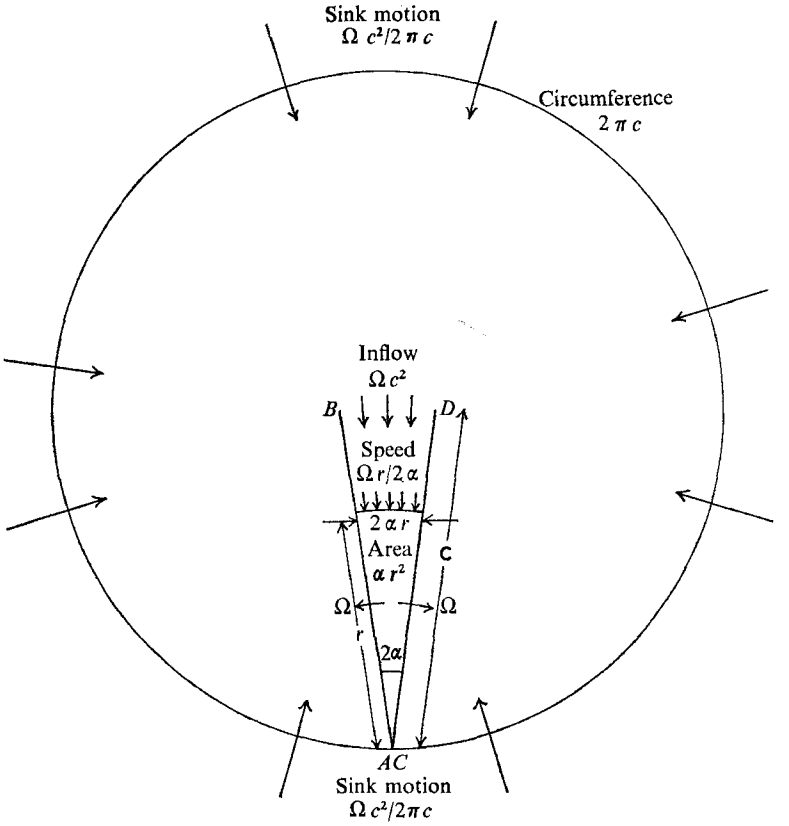

FIGURE 5. The initial stage of the 'fling' process. The area αr^2 of a sector of radius r and semi-angle α increases at a rate Ωr^2, which must be balanced by inflow across an arc of length $2\alpha r$ at a mean speed $\Omega r/2\alpha$. The external motion, on the other hand, is that due to a sink of strength Ωc^2 representing the inflow into BD.

model 'memory': in fact, it is modified by a distribution of vorticity that has been convected and diffused since first being shed from the boundary at a rate depending on how the boundary was moving the fluid at that time.

3. Modifications due to viscous effects

The inviscid-flow theory of § 2 predicts that, after the wings break apart, the fluid continues to move irrotationally (that is, without vorticity) but with circulations $\Omega_0 c^2 g(\alpha_0)$ around AB and CD in the negative and positive senses respectively. In this section we consider modifications to this conclusion, still on a two-dimensional model, due to shedding of vorticity from the wings both before and after they break apart.

If vorticity is shed from the boundary in a motion like that depicted in figure 2, the total flow field is the sum of (i) the irrotational flow (calculated in § 2) compatible with the boundary's motion normal to itself, and (ii) the flow field that the vorticity distribution would induce if the boundary were at rest. The modifying flow field (ii) can often be calculated by the method of images: in fact, when

the vorticity distribution is mapped into the Z plane of figure 3 with an infinite straight-line boundary, the associated flow field is that of the vorticity distribution plus that of a mirror-image distribution of equal strength and opposite sign.

The vorticity distribution in a two-dimensional flow is determined by the principles (i) that vorticity is subject to convection by the local fluid velocity and diffusion with diffusivity ν (the kinematic viscosity), and (ii) that the boundary is a source of vorticity (Lighthill 1963), which appears from it at the rate required to maintain the no-slip condition. In the problem of figure 2, for example, flow *changes* occurring in a short time interval leave the boundary condition on normal velocity undisturbed: the irrotational component changes at once to that associated with the new attitude α and angular velocity Ω of the boundary, while the previously existing vorticity distribution adopts after convection and diffusion a new configuration but, in combination with its image system, continues to make no alteration in the normal velocity at the boundary. All these changes, by contrast, perturb the tangential velocity at the boundary, so that the no-slip condition can be maintained only if new vorticity appears at the boundary in the form of a vortex sheet of strength equal to that perturbed tangential velocity: a vortex sheet which itself begins at once to be convected and diffused.

In certain circumstances its *convection* may be essentially tangential so that all the vorticity generated remains close to the boundary, filling after time t a boundary layer with thickness proportional to a diffusion length $(\nu t)^{\frac{1}{2}}$. This is particularly the case wherever the irrotational component of flow involves accelerating motions close to the boundary, so that the source of vorticity must always be of one sign: that which permits the slip across the boundary layer to increase. For example, on the lower surfaces of the wings in figure 2, such an accelerating motion is found. Initially, when α is small (figure 5), it is an accelerating 'sink' flow into the opening orifice BD. For all α, however, the velocity calculated by the irrotational-flow theory of § 2 increases along the lower surface of each wing even for fixed angular velocity Ω, while the fluid's acceleration is even more pronounced when Ω is increasing with time.

This is important because, when α has risen to values around $\frac{1}{3}\pi$ where the wings break apart, about half of the total circulation $\Omega c^2 g(\alpha)$ predicted in §2 (with $g(\alpha)$ in the 'flat' region of figure 4) for the circulation round each wing comes from the underside. This part, as a contribution to the circulation round the wing and the attached boundary layer, is not significantly modified, then, by viscous effects.

By contrast, wherever the irrotational component of flow involves decelerating motions close to the boundary, the vorticity required to allow its slip over the boundary decreases, which demands the generation at the boundary of vorticity of opposite sign. When that becomes sufficient to counteract diffusion of previously existing vorticity towards the surface, a reversed flow results near the surface which combines with forward flow in the region of accelerating motions to cause movement of fluid away from the surface. Such flow *separation* may convect vorticity to a much greater distance from the surface in a given time t than pure diffusion could.

Irrotational motions involving substantial flows around a wing leading edge that is sharp or has relatively small radius of curvature are classic cases where the tangential velocity accelerates up to the edge and then decelerates, commonly leading to reversed flow beyond the edge. Then the flow may separate from the edge, the associated convection of vorticity being known as leading-edge vortex shedding. Cases exist when that vorticity moves far away from the surface, facilitating a complete flow separation with fluid on rounding the leading edge moving far from the surface (as in a stalled aerofoil flow). In other cases it is forced back onto the upper surface, enclosing a 'leading-edge bubble' of separated flow of relatively modest dimensions. This can happen in steady flow, and happens still more commonly in starting flows generated by a wing's movement over only a moderate distance compared with its chord.

A leading-edge bubble is particularly to be expected in the flow of figure 2. At the leading edge of each wing the tangential velocity rises to a maximum and then sharply decelerates, making flow separation practically certain. In the early phase depicted in figure 5, however, the equation of continuity demands that the total fluid motion be sucked into the opening gap, carrying with it the vorticity. This convective effect greatly limits the potentiality for shed vorticity to move far from the boundary. At the same time diffusive effects in that opening region may reduce the strength of the vorticity of opposite sign to the right and left of the line of symmetry by diffusive flux across it.

When the wings break apart, the leading edges have each travelled about one chord length through the fluid, and vorticity shed in the early stages has been sucked into the opening gap, some of this being destroyed by diffusive action. This makes it probable that most of the shed vorticity which remains is confined to a bubble-shaped region attached to the leading edge, enclosing a relatively short region of reversed flow. The low Reynolds number (around 30) of the motions of *Encarsia formosa* would certainly help to promote bubble reattachment by increasing diffusive effects: at high Reynolds number it is known that laminar-separation bubbles from the leading edges of aerofoils are particularly prone to reattachment when transition to turbulence takes place in the separated boundary layer, essentially because that transition enhances diffusion; the analogous enhancement of diffusion at Reynolds numbers around 30 can be expected to have a similar effect.

Such a leading-edge bubble would not impede the operation of the Weis-Fogh mechanism. When the wings move apart as in figures 1 (*f*), (*g*) and (*h*) the immediate development of a high lift coefficient would indeed be facilitated by the effective rounding of the leading edge to a 'good aerofoil section' provided by the bubble.

Furthermore, the circulation around the effective aerofoil consisting of wing and bubble would be enhanced, if anything, be the bubble's presence. Figure 6 sketches possible shapes (whose accuracy or otherwise is not important) for the vortex sheet round the bubble in both the z plane and the Z plane of figure 3. In the Z plane the equal and opposite image vorticity in the straight-line boundary is also shown: the complex potential w in that plane is equal to the irrotational-flow value (8) plus the potentials of the vorticity distribution and its image

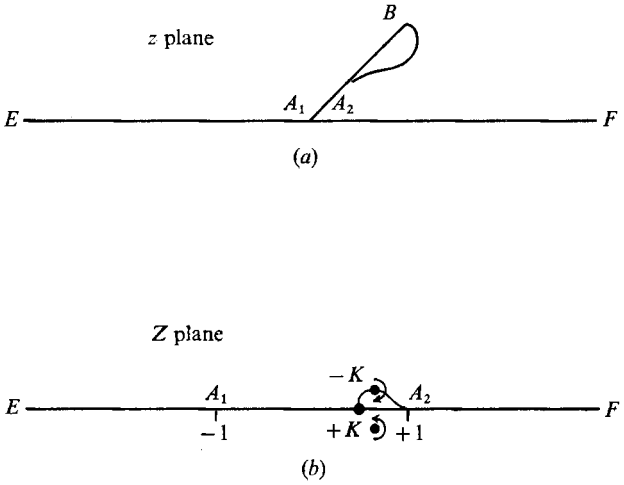

FIGURE 6. Possible shape of a vortex sheet enclosing a leading-edge bubble in (*a*) the z plane and (*b*) the Z plane (compare figure 3). In the Z plane the position suitable for a line vortex used to estimate its effect on Γ is also shown, together with the image position.

distribution. The circulation round the wing and the bubble from A_1 to A_2 is the change in velocity potential ϕ from $Z = -1$ to $Z = +1$ round a path lying above all those vortices, and is increased above its irrotational-flow value (1) by a slightly larger contribution from the negative vorticity in the upper half-plane than from the positive image vorticity in the lower half-plane.

To see that this effect, if present, would however be small, we may consider the influence of a single vortex of strength $-K$ at the point $Z = l + im$ (figure 6). The irrotational-flow velocity in the Z plane has in $-1 < Z < 1$ an average value $\frac{1}{2}\Gamma$ since Γ is its integral from -1 to 1, so that the postulated vortex at $Z = l + im$ and its image at $Z = l - im$ are of the right order of magnitude to reverse the flow if $K/\pi m = \frac{1}{2}\Gamma$. But the additional circulation round a contour going from -1 to $+1$ above the vortex is

$$\frac{K}{\pi}\left[\tan^{-1}\left(\frac{m}{1-l}\right) + \tan^{-1}\left(\frac{m}{1+l}\right)\right], \tag{14}$$

which is of order of magnitude

$$\Gamma m^2/(1-l^2) \ll \Gamma. \tag{15}$$

Similar conclusions result from consideration of vorticity distributed in a sheet around a bubble. They are analogous to the classical prediction of a slight enhancement of circulation round a two-dimensional aerofoil in steady flow at given angle of incidence due to increased aerofoil thickness; and they might like that be cancelled out in practice by other effects.

We also consider briefly any vortex shedding after the wings move apart. Note first that such trailing-edge vortex shedding as results in unsteady aerofoil theory from pressure inequalities at the trailing edge is not expected initially in the flow of figure 1(*f*), where the pressures on the two sides of the opening gap are approximately equal.

Initially, then, the flow over the upper surface of the wing AB can continue along lines depicted in figure 6 (a) as an ordinary aerofoil flow with a leading-edge bubble. Continued reattachment of the upper-surface flow is influenced favourably by translational acceleration of the wing surface. Admittedly, on the lower surface, the cessation of wing rotation and adoption of a translational mode of motion imply a change in sign of the surface's tangential motion relative to the external fluid. A new boundary layer typical of flow over the lower surface of an aerofoil must at once be formed. Its positive vorticity must more than overcome the already existing negative vorticity in the boundary layer associated with the external flow calculated in § 2, to such an extent that the *total* vorticity takes the positive value that permits the required slip between the lower surface and the external fluid. Actually, no special difficulties arise in boundary layers associated with solid surfaces whose tangential motion relative to the fluid changes sign in this way (compare the well-known Stokes layers involving periodic changes in sign): the diffusion helps to produce gradually a cancelling of negative and positive vorticity but at each instant it is in any case only the total vorticity in the layer which significantly influences the external flow.

As the translational motion proceeds, say with velocity U, the circulation Γ may change owing to gradual vortex shedding at the trailing edge, but it will stay constant if $\Gamma = \frac{1}{2}UcC_L$, where C_L is the value of the lift coefficient for wing motion through the ambient fluid at the angle of incidence in question† with *zero net vortex shedding* (the viscous-flow generalization of the Kutta–Zhukovski condition). This determines a value of U such that the full steady-flow lift per unit span

$$\rho U\Gamma = \tfrac{1}{2}\rho U^2 cC_L \tag{16}$$

can be realized from the outset. This possible implication, a total absence of the Wagner effect, is further explored in § 4.

4. Conclusion

Weis-Fogh (1973) described the zoological implications of his mechanism of lift generation regarding which aerodynamical details have been worked out in the present paper. We may conclude with a broader aerodynamic perspective of its method of working.

In terms of a purely two-dimensional flow (figure 1) the 'fling' allows the wings immediately after they break apart to experience something close to maximum lift, essentially because in the language of the Prandtl–Wagner theory each acts as a 'starting vortex' for the other: one of full strength, indeed, rather than the half strength of Wagner's classical starting vortex (Wagner 1925). The concentration of fluid vorticity into two 'bound vortices' (that is, the vorticity attached to a wing in boundary layers, leading-edge bubbles, etc., all adding up to the circulation round it) implies that the fluid impulse downwards, which is the *moment* of the distribution of horizontal vorticity, has a constant rate of increase, generating by reaction a constant lift.

† The effective angle of incidence is, however, less than the geometrical angle of each wing to the horizontal because (§4) each wing moves in the 'downwash' from the other.

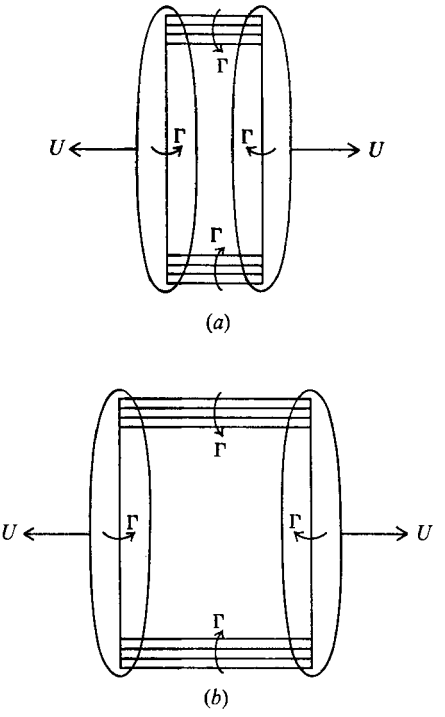

FIGURE 7. Schematic diagram of the Weis-Fogh mechanism for wings of finite span in rectilinear motion. The instantaneous generation of the circulation Γ round each wing by the 'fling' process is necessarily accompanied as in position (*a*) by the generation of tip vorticity with the same total circulation round it, which then grows by the usual process of tip-vortex shedding as in position (*b*).

The problem of fitting the local, approximately two-dimensional motions studied in §§ 2 and 3 into a fully three-dimensional model of the flow around real wings of finite span can be tackled by the classical methods of Prandtl (1918). We indicate this first in a case as close as possible to those studied by Prandtl, considering parallel straight wings of finite span in *rectilinear* motion away from one another, which at each cross-section along the span takes the form illustrated in figure 1.

Then the mechanism studied in §§ 2 and 3 for generating circulation around each wing cross-section works to produce bound vorticity of opposite signs on the two wings of figure 1: 'into the paper' on the left-hand wing and out from it on the right. The full three-dimensional pattern of vorticity must, however, be solenoidal: that is, the vortex lines must close up, which as in Prandtl's theory requires the presence of tip vortices (figure 7). These must be generated simultaneously with the circulations and be of sufficient strength to carry all the bound vorticity on the left-hand wing round through 180° at the wing tips and back into the right-hand wing.

The flow near the wing tips as the circulation and this associated tip vorticity are being formed can be inferred from the directions of the tip vorticity vectors in figure 7 (*a*) as a flow *inboard* from the tips in the region above the wings, and

a corresponding flow outboard to the tips in the region below them. The flow inboard can be regarded in the early stages of the 'fling' motion as a spanwise inflow into the opening gaps. Of course, the opening of mid-span wing sections can suck in air most readily in the plane of those sections as in figure 5; near the tips, however, the sucking can produce significant inboard motion that represents part of the local flow pattern associated with the generation of tip vortices.

Figure 7 (*b*) shows as the wings move apart the equal and opposite bound vorticity on each joined continually by tip vortices so as to keep the whole vorticity field solenoidal. They become longer by the usual mechanism that causes lifting wings to shed tip vorticity: pressure excess on the lower surface pushes fluid outboard near the tips, while pressure defects on the upper surface suck fluid inboard, to generate flow twist near the tips about the wing's direction of motion. In the meantime the fluid impulse downward, which is the moment of the distribution of horizontal vorticity (for example, circulation times area in the use of a single closed line vortex), has a constant rate of increase, generating by reaction a constant lift.

The three-dimensional flow pattern of figure 7 can be expected to modify in some degree the two-dimensional motions around mid-span sections through essentially the same mechanism as in Prandtl's theory: the effective motion of each section is not through 'otherwise undisturbed' fluid, but through fluid subjected to a 'downdraught' or 'downwash' induced by the full three-dimensional pattern of vorticity. As a result, each wing section possesses an effective angle of incidence less than its geometric angle of incidence by an amount equal to the ratio of downwash to wing speed.

Such a downwash correction, indeed, in *unsteady* aerodynamic problems (including the problem of this paper), is present even when they are treated two-dimensionally: for example, the Wagner effect can be thought of as due in part to reduction of the effective angle of incidence through downwash induced by the starting vortex. The Weis-Fogh mechanism involves a similar reduction, as remarked in a footnote at the end of § 3, because each wings moves in the downwash field of the other wing's bound vorticity. There is, however, no resulting loss of lift in this latter case, since the circulation about the wing section has been fixed independently by the 'fling' motion. The reduction means only that relatively high geometric angles of incidence (for example, 30° according to figure 1) are appropriate as the wings first move apart (and are achievable without the wings stalling). Note, furthermore, that the three-dimensional vortex pattern of figure 7, acting together perhaps with some vorticity generated in earlier wing beats, somewhat increases the induced downdraught at each wing section above the value suggested on two-dimensional flow theory.

The wings of *Encarsia formosa*, of course, do not adopt the simple rectilinear motion of figure 7: their tips describe, as explained in § 1, a circular path around the erect body. This must bring into being a tip vortex in the form of a growing circular arc to close the vortex lines. This important consequence of the circulation set up round the wings is shown in figure 8 together with the 'inboard vortex': a much shorter circular-arc vortex close to the body, required to close the vortex lines in that region. Figure 8 shows a linear growth in the area enclosed by vortex

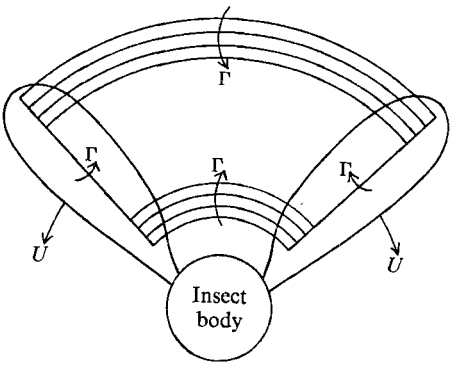

FIGURE 8. Schematic diagram of the outboard and inboard circular-arc tip vortices in the hovering flight of an insect moving its wings in a horizontal circle about its erect body.

lines and hence in the downward impulse of the vorticity distribution, corresponding to a constant lift as before. Its value is independent of induced downwash effects, which again influence only the local angles of incidence.

It is arguable that the fullest possible utilization of the Weis-Fogh mechanism would be one in which the animal could continue the movement of both wing tips circumferentially as in figure 8, but through the total angle of 180°, making the full 'clap and fling' motion twice per beat instead of once as in *Encarsia formosa*. Then when the circular-arc tip vortex of figure 8 had grown into a complete downward-moving vortex ring the 'clap' would take place and blow the loose ends downwards clear of the body,† to level up the whole vortex ring (whose diametrically opposite side had begun its descent earlier). Then another 'fling' would occur, generating new circulation of opposite sign around the wings, which as they moved back in the opposite direction would create a further complete vortex ring of the *same* sign as before.

This picture of an 'ideal' utilization of the Weis-Fogh mechanism leading to the support of an animal's weight by momentum generation in the form of a sequence of downward-moving circular vortex rings, two per wing beat, is of some theoretical interest because the circular shape of vortex line carries the greatest possible momentum (proportional to the area enclosed) per unit kinetic energy. We may note incidentally that, far below the animal, viscous dissipation of energy flux without change of momentum flux would gradually convert that motion into the classical 'laminar round jet' solution of the equations of motion (Landau 1944; Squire 1951) corresponding to the action of a point source of momentum in a viscous fluid. Indeed, the flow field far below any small enough hovering animal of mass m must take the form of this similarity solution, depending on just one parameter: the ratio between the force mg with which the animal acts on the fluid and the quantity $\rho\nu^2$ of the same dimensions formed from the fluid's density ρ and kinematic viscosity ν. The ratio (a sort of Reynolds

† Note that the air motion during the 'clap' is not the reverse of that during the 'fling': evidently, the outflow from the closing gap, far from being an irrotational source-type motion (the reverse of the sink-type motion of figure 5) is a separated efflux in the form of a downward-pointing jet.

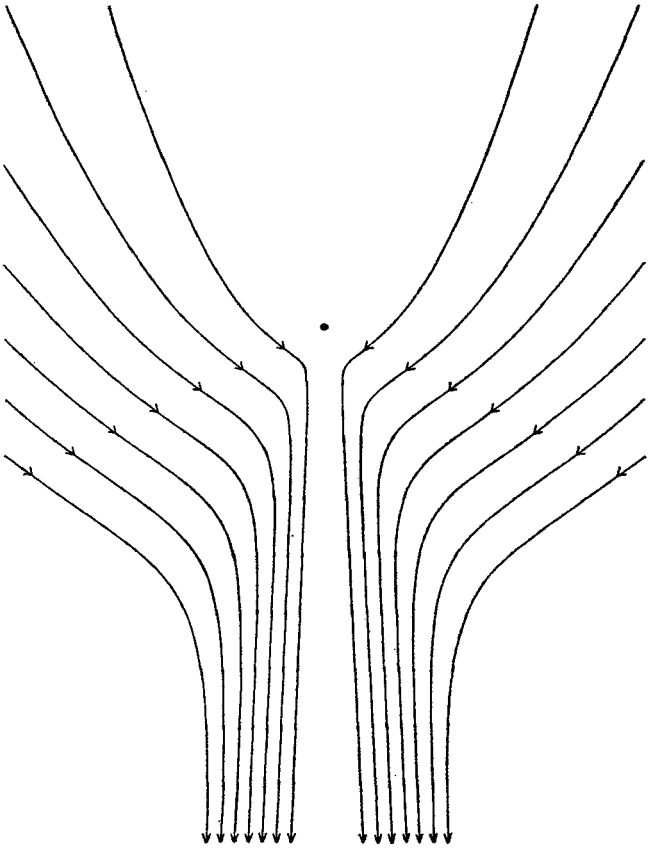

FIGURE 9. Streamlines in the far flow field due to the delivery by *Encarsia formosa* of downward momentum mg per unit time at the marked position to air of kinematic viscosity ν and density ρ, where $mg/\rho\nu^2 = 900$. Streamlines are plotted at equal intervals of Stokes's stream function.

number *squared*) is around 900 for *Encarsia formosa* (with $m = 0{\cdot}025$ mg): quite small enough for the associated downward jet-type far-field flow (see figure 9) to be extremely stable.

Encarsia, admittedly, is not able to move its wings through the full angle of 180° so as to perform a true 'clap and fling' *twice* (as suggested in the last paragraph but one) per beat: they can move, in fact, through only about 130°. Subject to this limitation, however, it can be argued that its motions approximate as closely as is feasible to those described above. It does a complete 'clap and fling' at one extreme of every wing beat, and makes at the other extreme a broadly similar 'flip' motion (with the same total magnitude of wing angular movement), harder to analyse and without bringing the two wings together. Quite possibly the combination may give advantages not too far from what the 'ideal' motion would achieve!

REFERENCES

LANDAU, L. D. 1944 *Dokl. Akad. Nauk. SSSR*, **43**, 286.

LIGHTHILL, M. J. 1963 In *Laminar Boundary Layers* (ed. L. Rosenhead), chap. 2, §1.7. Oxford University Press.

PRANDTL, L. 1918 Tragflügeltheorie. *Nachr. Ges. Wiss. Göttingen*, pp. 107, 451.

SQUIRE, H. B. 1951 *Quart. J. Mech. Appl. Math.* **4**, 321.

WAGNER, H. 1925 *Z. angew. Math. Mech.* **5**, 17.

WEIS-FOGH, T. 1973 *J. Exp. Biol.* (to appear).